



Cansmart 2008

International Workshop

SMART MATERIALS AND STRUCTURES

23 - 24 October 2008, Montreal, Quebec, Canada

**EXPERIMENTAL INVESTIGATION ON THE SEISMIC
PERFORMANCE OF SMA-FRP RC SMART BEAM-COLUMN JOINT**

M. Shahria Alam¹, Moncef Nehdi², Maged A. Youssef³

¹PhD Candidate, Department of Civil & Environmental Engineering, University of Western Ontario,
malam8@uwo.ca

²Professor, Department of Civil & Environmental Engineering, University of Western Ontario,
mnehdi@eng.uwo.ca

³Assoc. Prof., Department of Civil & Environmental Engineering, University of Western Ontario,
myoussef@eng.uwo.ca

ABSTRACT

The use of Fibre Reinforced Polymer (FRP) as reinforcement in concrete structures has received much attention owing to its higher resistance to corrosion compared to that of regular steel reinforcement, and has been a very active research area for the last two decades. Since FRP is a brittle material, ductility is considered as a major concern for FRP-reinforced concrete (RC) structures. Ductility of FRP RC structures can be achieved in conjunction with a ductile material such as steel, or shape memory alloy (SMA) which can be placed at the plastic hinge regions of a structure, while FRP bars can be used in the other regions of the structure. However, the use of steel involves the risk of corrosion. Nickel-Titanium (Ni-Ti) SMA is highly resistant to corrosion. If superelastic Ni-Ti can be used as reinforcement, it brings about added advantage in seismic regions since it has the ability to undergo large deformation, but can regain its undeformed shape through stress removal. In this research, beam-column joints reinforced with superelastic Ni-Ti SMA rebar at the plastic hinge regions of the beam and FRP in other regions of the beam and column have been tested under reversed cyclic loading. The results are compared in terms of load-storey drift and energy dissipation capacity to those of a similar RC beam-column joint specimen reinforced with conventional steel. eventually help in eliminating the majority of infrastructure management problems.

Keywords: FRP, SMA, Superelasticity, Corrosion, Ductility, Reversed Cyclic Loading.

INTRODUCTION

It has been more than hundred years since steel has been used as reinforcement for concrete structures. However, corrosion of steel is one of the major problems, which is responsible for early deterioration of reinforced concrete (RC) structures. Every year billions of dollars are spent for the rehabilitation of infrastructures especially for the replacement of corroded steel. In order to mitigate such problems, fibre reinforced polymer (FRP) bars have been introduced as reinforcement for concrete. Since FRP is a brittle material, ductility is the main problem associated with the FRP RC structures. Therefore, the use of FRP in RC structures still remains to be of great concern, especially, in seismic regions where ductility is one of the most important design criteria. Although steel (within its elastic range) and FRP RC elements are expected to behave in similar fashion as their behaviour basically depend on the bonding between rebar and concrete, low modulus of elasticity of FRP is responsible for causing larger deflection compared to that of steel RC elements. Again, absence of yielding and inelastic branch in the stress-strain behaviour of FRP will result in a sudden and brittle failure without adequate warning. Consequently, such FRP RC elements are often overdesigned in order to avoid rupture of FRP bars and increase safety of the structure.

Various researches are going on all around the globe in order to improve ductility of FRP RC elements (Nehdi and Said 2005, Won and Park 2006). Ductility of such structures can be achieved in conjunction with a ductile material e.g. steel, stainless-steel or shape memory alloy etc. which can be placed at the plastic hinge regions of a structure whereas FRP bars will be used in the other regions of the structure. Owing to the corrosion problem, steel can be discarded; instead stainless steel can be taken into consideration. Shape memory alloy (SMA) is another material, highly resistant to corrosion and superelastic SMA is a unique alloy with the ability to undergo large deformation, but can regain its undeformed shape through stress removal. In the case of using stainless steel along with FRP bar, this will positively reduce the maintenance cost since there will be no significant corrosion. However, it will experience significant permanent deformation under a large earthquake and will not be serviceable. On the other hand, use of SMA as reinforcement will not only eliminate the corrosion problem but also recover inelastic deformation at the end of earthquakes. Nevertheless, stainless steel is less costly compared to SMA.

Little research has been directed towards splicing of FRP rebar with another ductile material and use of such spliced connections in a beam-column joint so as to make the structure ductile with enhanced deformation capacity. In this study, a suitable coupler has been developed for splicing FRP with SMA rebar, and then the spliced FRP-SMA rebar was used as reinforcement in the beam-column joint. The prime objective of this study is to investigate the seismic behaviour of a concrete BCJ reinforced with SE SMA in its plastic hinge zone and FRP in other regions, and compare its performance to that of a regular steel RC BCJ in terms of load-displacement and energy dissipation capacity.

EXPERIMENTAL PROGRAM

A large-scale BCJ specimen was constructed and tested at the Structures Laboratory of the University of Western Ontario. The specimen (JBC-4) was reinforced with SE SMA at

the plastic hinge region of the beam along with GFRP rebar in the remaining portion of the joint.

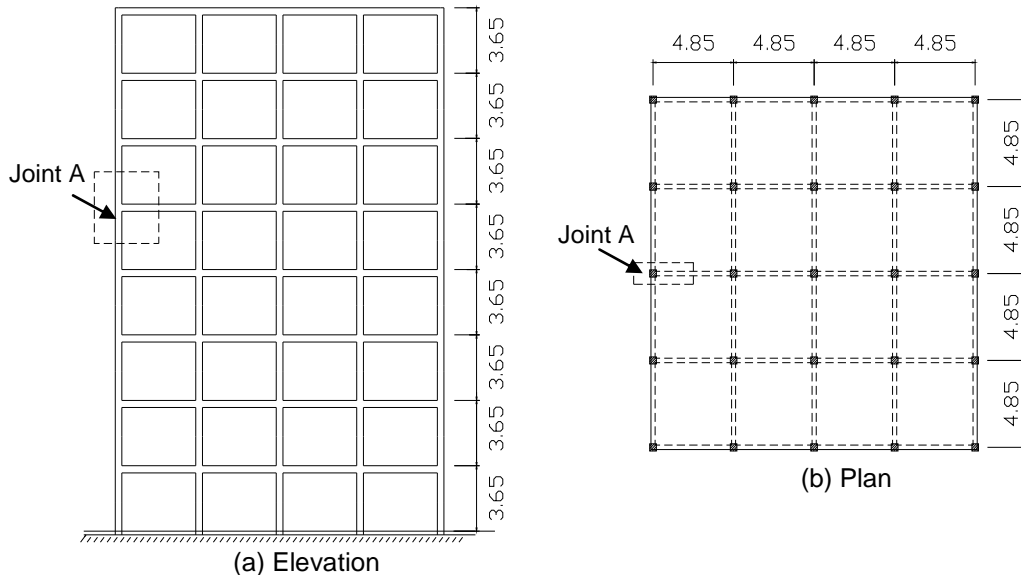


Fig. 1: Eight-storey frame building located in the western part of Canada (in meters).

An eight-storey RC building with moment resisting frames was considered in this study, which was assumed to be located in the western part of Canada on firm ground with undrained shear strength of more than 100 kPa. The elevation and plan of the building are shown in Fig. 1. It was designed and detailed in accordance with Canadian Standards¹¹. The design Peak Ground Acceleration (PGA) was 0.54g and the moment frames were designed with a moderate level of ductility. An exterior BCJ was isolated at the points of contraflexure, from mid-height of fifth floor to mid-height of sixth floor (Joint A in Fig. 1). The size of the BCJ test specimen was reduced by a factor of $\frac{3}{4}$ to account for the laboratory space and limitations of testing equipments. The forces acting on the joint were also scaled down by a factor of $(\frac{3}{4})^2$. This factor was chosen to maintain normal stresses in the scaled models similar to that of the full-scale joint.

Specimen Details

First the frame was analyzed considering all possible load combinations. Based on the analysis results, the beam and column of JBC-4 were designed for maximum moments and shear forces. The design column axial force, P , was 620 kN leading to a scaled down P of 350 kN. The detailed design of joint JBC-4 is given in Fig. 2. The top and bottom longitudinal reinforcement for the beam are 2-GFRP20 (19 mm in diameter) rebars and 2-SE SMA20 (20.6 mm in diameter) rebars at different section as shown in Fig. 2. The plastic hinge length was calculated as 360 mm (Paulay and Priestley 1992) from the face of the column. Mechanical couplers were used to connect SMA rebars and regular steel rebars. The total length of SMA rebars was 450 mm (centre to centre of the couplers). The size of the longitudinal rebar and the size and spacing of the transverse reinforcement for the joint conform to current code requirements (CSA A23.3-04).

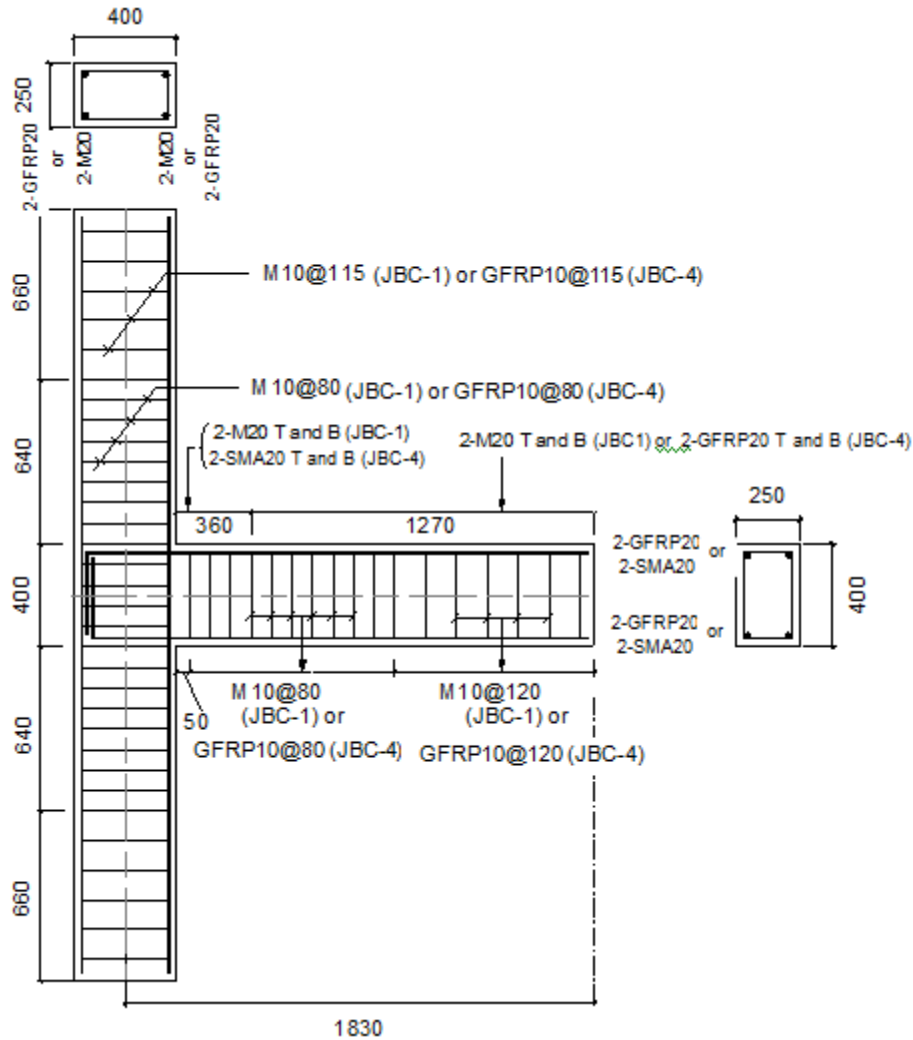


Fig. 2: Reinforcement details of specimen JBC-4 along with JBC-1(in mm).

Splicing Technique

Splicing of FRP rebar with another ductile material like SMA rebar was one of the major challenges for this experimental program. There was no mechanical coupler readily available in the market that can connect brittle FRP rebar with another ductile material. Regular screw-lock coupler was tested for splicing and it was found that the sharp end of the screw ruptures the top fibres of GFRP rebar. Flattened screws were also used but did not work as the FRP rebar was not strong to take normal forces in the perpendicular direction of the orientation of fibres and the fibres get easily damaged. Therefore, the only option was to use adhesive type coupler for the sand coated FRP bar.

Adhesive type coupler was also tested for connecting SMA rebar. Since this type of coupler resists the force solely by friction, SMA rebar slipped out easily while it was being pulled because of its smooth surface. Therefore, it was necessary to look for mechanical anchorages. Machining large diameter bars of Ni-Ti using conventional equipment and techniques is extremely difficult due to its high hardness. Although there are various ways of welding and soldering Ni-Ti, e.g. using e-beam, laser, resistance and friction welding, and

brazing with Ag-based filler metals; welding Ni-Ti to steel coupler is much more problematic because of the development of a brittle connection around the weld zone (Hall 2003). Weld deposits with Ni-filler metal have exhibited sufficient tensile strength allowing SE deformation of Nitinol (Hall 2003). Threading large diameter nitinol bars reduces its strength due to its sensitivity to notches. Therefore, instead of threaded couplers, bar lock couplers with flat shear bolts have been used. Several couplers were tested with SMA rebar having variable number of screws and different arrangements and was found that nine-5 mm diameter flat end screws arranged in three rows were adequate to minimize the relative slippage between the rebar and the coupler. Finally, the coupler that was used in the specimen JBC4 had two parts: one was a stainless steel pipe filled with epoxy resin for holding FRP rebar and the other one was screw-lock coupler for holding SMA rebar as shown in Fig. 3 and is named as screw lock-adhesive type coupler.

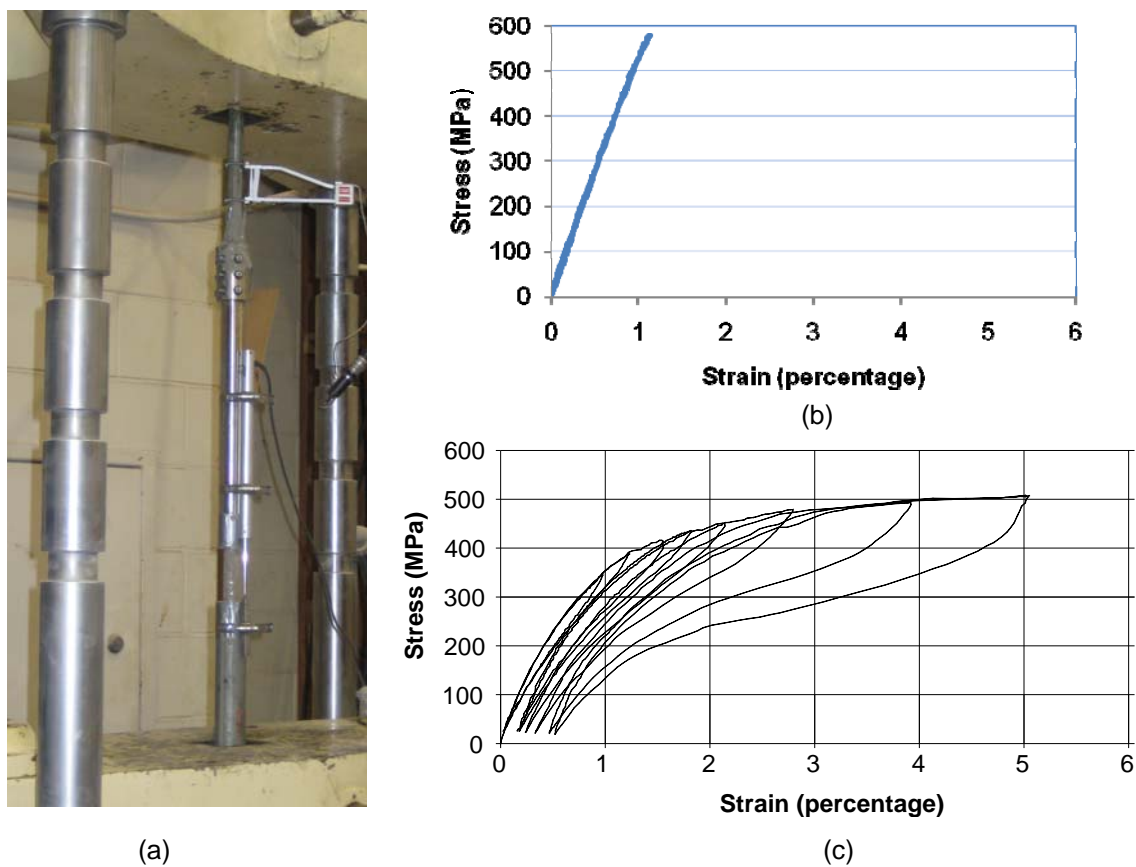


Fig. 3: (a) Testing of the splice connection of FRP and SMA using screw lock-adhesive type coupler in the universal testing machine, (b) cyclic tensile strength of SE SMA rebar within couplers, and (c) cyclic tensile strength of GFRP rebar within couplers.

Specimen Details

The concrete used for casting the specimen had a compressive strength of 45.7 MPa at the time of testing. The split cylinder tensile strength 3.0 MPa. In this project, glass fibre reinforced polymer (GFRP) rebar (also known as V-Rod) was used, which was manufactured by Pultrall Inc., Canada. The surface of the rebar was sand coated so as to improve the

bonding between concrete and FRP. The binding material of FRP rebar is composed of modified vinyl ester resin with a maximum volume fraction of 35 percent along with continuous e-glass fibers with a minimum volume fraction of 65 percent. The manufacturer's specified design tensile strength, ultimate strength and tensile modulus were 656 MPa, 728 MPa and 47.6 GPa, respectively. Its coefficient of thermal expansion was specified as $6 \times 10^{-6} / ^\circ\text{C}$. Cyclic tensile test was performed on the splice arrangement of FRP and SMA rebar in the universal testing machine as shown in Fig. 3. It was not possible to conduct the test up to the rupture of FRP rebar as the connection failed due to sliding of the FRP rebar from the coupler. The test result (Fig. 3b) shows that the connection failed by sliding out of FRP rebar at a stress of 577 MPa. The tensile modulus of FRP rebar was 52.2 GPa, which was higher than that of the specified value.

Hot-rolled Ni-Ti alloy rebar has been used as SMA reinforcement in JBC-4 specimen. The composition of all of the samples was nearly identical, with an average of 55.0% nickel and 45.0% titanium by weight. Its austenite finish temperature, A_f , defining the complete transformation from martensite to austenite, ranges from -15°C to -10°C . Above this temperature, the alloy is within the superelastic range. Each Ni-Ti bar used in this study was 450 mm long and 20.6 mm in diameter. Figure 3c shows the stress-strain behaviour of SMA while testing the SMA-FRP splice connection. This figure shows the cyclic tensile behaviour of SMA up to its superelastic strain of 5%, where the characteristic stress-strain curve shows a flag-shaped response. Although SMA does not have a yielding process, yield is being used in this study to refer to the initiation of phase transformation of SMA. The yield point is identified as 401 MPa ($f_{y, SMA}$) at 0.64% strain (ϵ_y) with a Young's modulus (E) of 62.5 GPa. This is to be noted that this yield strength has been defined from an idealized bilinear elastic-plastic SMA stress-strain model with kinematic strain hardening. Since the splice connection failed due to failure of FRP connection, the rebar was subjected to 5% strain at the time of failure, and a residual strain of 0.58% was observed.

Loading

While testing the BCJs, constant axial load was applied at the top of the column and reversed quasi-static cyclic load was applied at the beam tip. The load history applied at the beam tip was divided into two phases where a load-controlled phase was followed by a displacement-controlled loading phase. During the load-controlled phase, two load cycles were applied at 10% of the theoretical yield load of the beam to ensure that the data acquisition system is functioning properly. The following load control cycles (4 cycles) were applied to define the loads causing flexural cracking in the beam (2 cycles) and yielding of its longitudinal rebars (2 cycles). The yield load, P_y , and the yield displacement, Δ_y , were recorded. After yielding, displacement-controlled loading was applied. In order to verify a stable condition, for each load cycle the test specimen was subjected to two complete cycles. Tests were conducted up to a storey drift of at least 4%, which is more than the collapse limit defined by [Elnashai and Broderick \(1994\)](#).

Test Setup and Instrumentation

Figure 4 illustrates the schematic diagram of the specimen, the test rig, and the reaction frame. The bottom of the column was hinged with pins penetrating through a sleeve with

narrow holes. A roller support was created at the top of the column with pins penetrating through a sleeve with 20 mm vertical slots. The load cycles were applied at the beam tip using an actuator, which was pin connected at the beam-tip. The arm length was measured as 1870 mm from the pin connection to the mid column line. Figure 4 also illustrates the instrumentation of test specimens. Two load cells were used to measure the column axial load and beam tip load. During testing, displacements were measured at various locations using linear variable displacement transducers (LVDTs). One pair of LVDT was attached to the joint area to measure the joint distortion. The other two LVDTs were placed in parallel on top and bottom of the beam at a distance of 180 mm away from the column face to measure beam rotation. The displacement was measured at the free end of the beam using a string potentiometer. A portable computer attached to the data acquisition system was used to record readings at a constant time interval with one reading per second.

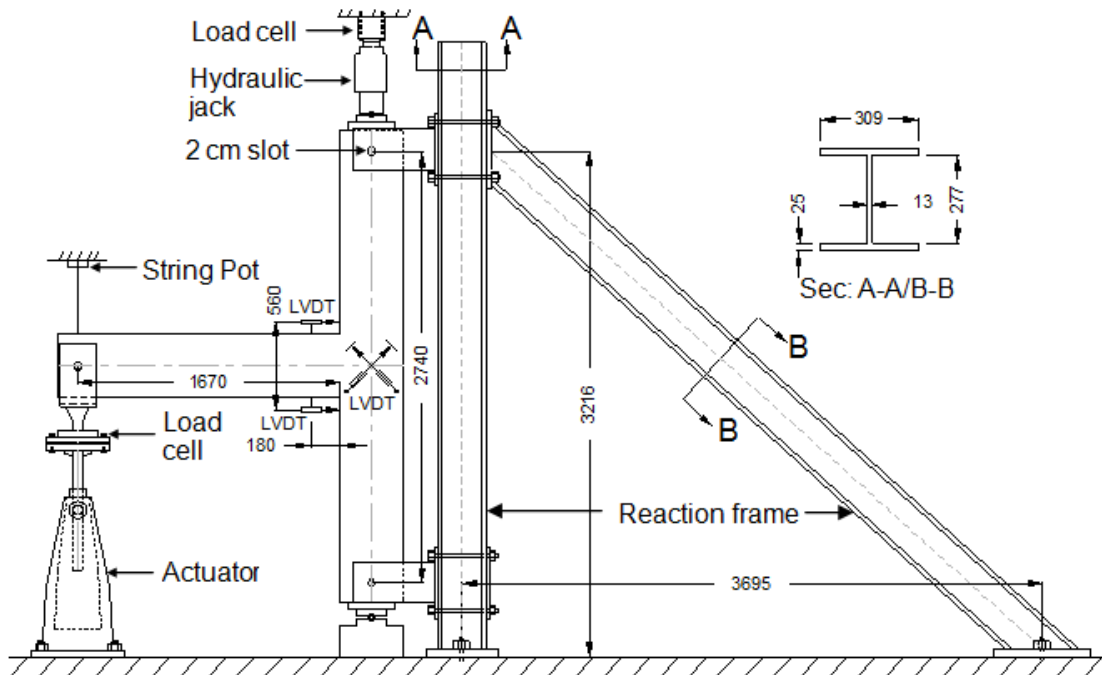


Fig. 4: Test setup (in mm).

EXPERIMENTAL RESULTS

Figure 5 shows the load-storey drift relationship of FRP-SMA RC beam-column joint specimen JBC-4. The First Flexural Crack (FFC) was detected at the bottom of the beam at 72 mm away from the column face at a drift of 0.22%. In the following cycle having the same drift; another crack developed at the top of the beam at a distance of 85 mm away from the column face and extended meeting the first crack. Thus, a single fine crack is formed that extended over the full beam-depth. With the progress of loading several flexural cracks occurred at the top and bottom of the beam along a length of 900 mm measured from the column face. At a drift of 0.66%, the FFC opened up to a width of 0.5 mm at the bottom but it could not fully close after unloading. A fine crack took place at the joint region at a beam tip-load of 26 kN corresponding to a drift of 0.99%. While subjected to a drift of 1.32%, the FFC opened up to 1.2 mm, where the residual crack width was zero after unloading. It was

observed that the bottom SMA rebar reached its yield strain at a beam tip-load of 34.1 kN and a drift of 1.97%. In this case, the corresponding yield displacement, Δ_y was found as 18 mm. At this stage the opening sizes of the FFC were 1.5 mm and 1.0 mm, where the residual crack widths were 0.1 mm and 0.05 mm at bottom and top, respectively. At a drift of 2.73%, a crack formed at the face of the column and propagated deeper into the beam. Some minor cracks also streamed out of the FFC toward the column face. The FFC also started to grow wider and reached a width of 3.6 mm at the outer face at a drift of 3.28%. When the displacement cycle reached a zero value, the FFC width became smaller and it was even less than 0.85 mm. At a drift of 4.4%, the FFC opened up to 5.4 mm and later closed to a width of less than 1.5 mm. The joint region exhibited few cracks of fine width and small length, and remained almost fully intact. Figure 6 shows the crack pattern of JBC-4.

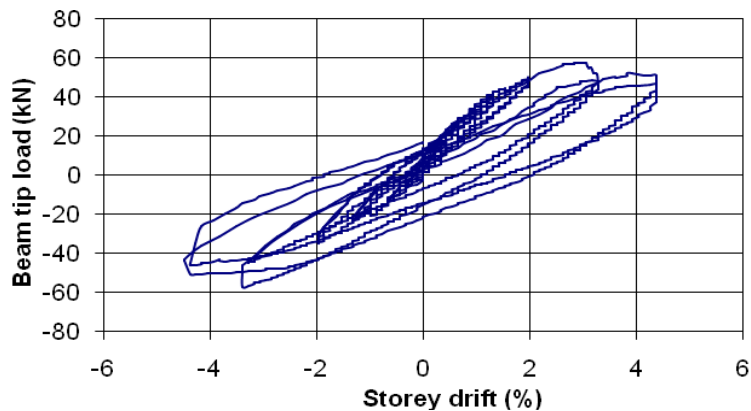


Fig. 5: Beam tip load-storey drift relationship of specimen JBC-4.



Fig. 6: Crack pattern of specimen JBC-4 after being subjected to reversed cyclic loading.

PERFORMANCE COMPARISON BETWEEN SMA-FRP AND STEEL RC BCJ

This section compares the performances of JBC-4 to that of JBC-1 ([Youssef et al. 2008](#)) in terms of load-displacement and energy dissipation capacity.

Load-Storey Drift Envelope

The beam-tip load versus storey drift envelope of both specimens JBC-1 and JBC-4 exhibited typical elasto-plastic behaviour as depicted in Fig. 7. Although they started with comparable stiffness, the FRP-SMA RC specimen experienced a drop in its stiffness after the first flexural crack was observed. This is because of SMA's lower Young's modulus compared to that of steel. However, both specimens showed similar load carrying capacity at a drift of about 3.0%. Beyond 3% drift, there was a slight decrease in tip load in case of JBC-4, which became flattened at 4% drift. At this stage, JBC-4 had 15% lower capacity compared to that of JBC-1. This is to be noted that even beyond 4% drift, JBC-4 could carry more than 50 kN of tip load.

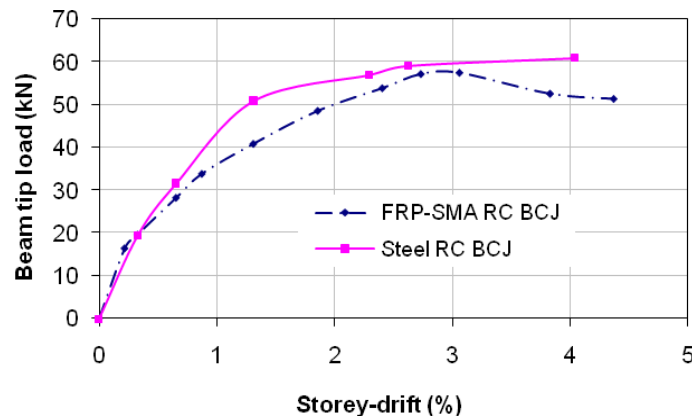


Fig. 7: Beam tip-load-storey drift envelope of specimens JBC1 and JBC4.

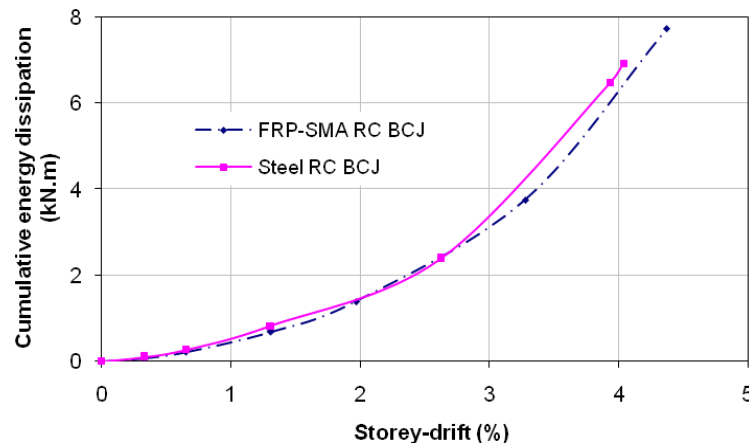


Fig. 8: Cumulative energy dissipation-storey drifts relationship of JBC1 and JBC4.

Cumulative Energy Dissipation Capacity

The cumulative energy dissipation with respect to storey drift for specimens JBC-1 and JBC-4 is depicted in Fig. 8. JBC-1 dissipated 3.4 kN.m of energy at a storey drift of 3% (collapse limit as defined by [Elnashai and Broderick 1994](#)), whereas JBC-4 dissipated 3.1 kN.m of energy. At a storey drift of 4%, JBC-4 dissipated 6.29 kN.m of energy, where JBC-1 dissipated 6.76 kN.m of energy, which is only 7.5% higher compared to that of JBC-4. The level of damage in JBC-4 indicates that the FRP-SMA RC joint suffered extensive cracking in the beam hinge region (Fig. 6), which helped to dissipate similar amount of energy

compared to that of JBC-1 where the steel RC joint dissipated energy through larger hysteretic loop of steel rebar compared to that of SE SMA rebar besides few smaller width cracks.

CONCLUSIONS

The use of SE SMA rebars in the plastic hinge region and FRP in other regions of a BCJ has been examined under reversed cyclic loading. The experimental investigation described in the present paper provides an insight into the potential for developing a new generation RC structures, which will be corrosion free as well as ductile. Based on the experimental observations and analysis of test results, the following conclusions can be drawn.

Coupled SE SMA-FRP rebar produced force-displacement hysteresis for JBC-4 with reduced stiffness and some residual drift. Although use of SMA at plastic hinge region was supposed to reduce residual drift significantly due to its superelasticity, the increased residual deformation might be due to significant slippage of FRP rebar inside the coupler. However, the specimen, JBC-4 could carry 89% of its full load carrying capacity beyond its collapse limit (4% drift). Such corrosion free ductile SMA-FRP RC structural elements could have a great benefit in highly corrosive environment, where such structures would remain functional with little or no maintenance/repairing. The use of SE SMA in the joint region of JBC-4 successfully relocated the plastic hinge region away from the column face to a distance of approximately one-quarter of the beam-depth. Specimen JBC-4 dissipated approximately same amount of energy compared to that of JBC-1. However, its energy dissipation was governed by extensive cracking of concrete.

REFERENCES

1. Nehdi, M. and Said, A., “[Performance of RC Frames with Hybrid Reinforcement under Reversed Cyclic Loading,](#)” *Materials and Structures*, 38, pp. 627-637, 2005.
2. Won, J.-P. And Park, C.-G., “[Effect of Environmental Exposure on the Mechanical and Bonding Properties of Hybrid FRP Reinforcing Bars for Concrete Structures,](#)” *Journal of Composite Materials*, 40(12) pp. 1063-76, 2006.
3. Paulay, T. and Priestley M.J.N., “[Seismic Design of Reinforced Concrete and Masonry Buildings,](#)” New York: J. Wiley, 1992.
4. CSA A23.3-04, “[Design of Concrete Structures,](#)” Canadian Standards Association, Rexdale, ON, Canada, 240p, 2004.
5. Hall, P.C. (2003) “[Laser Welding Nitinol to Stainless Steel,](#)” *Proc. of the International Conference on Shape Memory and Superelastic Technologies*, California, pp. 219-228.
6. Elnashai, A.S. and Broderick, B.M., “[Seismic resistance of composite beam-columns in multi-storey structures. Part 1: Experimental studies,](#)” *Journal of Constructional Steel Research*, 30(3), pp. 201-229, 1994.
7. Youssef, M.A., Alam, M.S. and Nehdi, M., “[Experimental Investigation on the Seismic Behaviour of Beam-Column Joints Reinforced with Superelastic Shape Memory Alloys,](#)” in press, *Journal of Earthquake Engineering*, accepted January 2008.